



HAL
open science

2 W / mm power density of an AlGa_N/Ga_N HEMT grown on free-standing Ga_N substrate at 40 GHz

Mohamed-Reda Irekti, Marie Leseq, N. Defrance, Etienne Okada, Eric Frayssinet, Yvon Cordier, Jean-Guy Tartarin, Jean-Claude de Jaeger

► To cite this version:

Mohamed-Reda Irekti, Marie Leseq, N. Defrance, Etienne Okada, Eric Frayssinet, et al.. 2 W / mm power density of an AlGa_N/Ga_N HEMT grown on free-standing Ga_N substrate at 40 GHz. Semiconductor Science and Technology, 2019, 34 (12), pp.12LT01. 10.1088/1361-6641/ab4e74 . hal-02929065

HAL Id: hal-02929065

<https://hal.science/hal-02929065v1>

Submitted on 11 Dec 2020

HAL is a multi-disciplinary open access archive for the deposit and dissemination of scientific research documents, whether they are published or not. The documents may come from teaching and research institutions in France or abroad, or from public or private research centers.

L'archive ouverte pluridisciplinaire **HAL**, est destinée au dépôt et à la diffusion de documents scientifiques de niveau recherche, publiés ou non, émanant des établissements d'enseignement et de recherche français ou étrangers, des laboratoires publics ou privés.

ACCEPTED MANUSCRIPT

2 W/mm power density of an AlGaIn/GaN HEMT grown on Free-Standing GaN Substrate at 40 GHz

To cite this article before publication: Mohamed-Reda IREKTI *et al* 2019 *Semicond. Sci. Technol.* in press <https://doi.org/10.1088/1361-6641/ab4e74>

Manuscript version: Accepted Manuscript

Accepted Manuscript is “the version of the article accepted for publication including all changes made as a result of the peer review process, and which may also include the addition to the article by IOP Publishing of a header, an article ID, a cover sheet and/or an ‘Accepted Manuscript’ watermark, but excluding any other editing, typesetting or other changes made by IOP Publishing and/or its licensors”

This Accepted Manuscript is © 2019 IOP Publishing Ltd.

During the embargo period (the 12 month period from the publication of the Version of Record of this article), the Accepted Manuscript is fully protected by copyright and cannot be reused or reposted elsewhere.

As the Version of Record of this article is going to be / has been published on a subscription basis, this Accepted Manuscript is available for reuse under a CC BY-NC-ND 3.0 licence after the 12 month embargo period.

After the embargo period, everyone is permitted to use copy and redistribute this article for non-commercial purposes only, provided that they adhere to all the terms of the licence <https://creativecommons.org/licenses/by-nc-nd/3.0>

Although reasonable endeavours have been taken to obtain all necessary permissions from third parties to include their copyrighted content within this article, their full citation and copyright line may not be present in this Accepted Manuscript version. Before using any content from this article, please refer to the Version of Record on IOPscience once published for full citation and copyright details, as permissions will likely be required. All third party content is fully copyright protected, unless specifically stated otherwise in the figure caption in the Version of Record.

View the [article online](#) for updates and enhancements.

2 W/mm power density of an AlGaN/GaN HEMT grown on Free-Standing GaN Substrate at 40 GHz

Mohamed-Reda Irekti^{1,2}, Marie Lesecq¹, Nicolas Defrance¹, Etienne Okada¹, Eric Frayssinet³, Yvon Cordier³, Jean-Guy Tartarin² and Jean-Claude De Jaeger¹

¹ Microwave Power Devices Group Institut d'Electronique, de Microélectronique et de Nanotechnologie, University of Lille, Villeneuve d'Ascq 59652, France

² Laboratoire d'Analyse et d'Architecture des Systèmes, Centre National de la Recherche Scientifique, Toulouse 31400, France.

³ Université Côte d'Azur, CNRS, Centre de Recherche sur l'Hétéro-Epitaxie et ses Applications, Valbonne 06560, France.

E-mail: mohamedreda.irekti.etu@univ-lille.fr

Received xxxxxx

Accepted for publication xxxxxx

Published xxxxxx

Abstract

In this letter, a record performance at 40 GHz obtained on AlGaN/GaN high electron mobility transistor (HEMT) grown on Hydride Vapor Phase Epitaxy (HVPE) Free-Standing GaN substrate is reported. An output power density of $2 \text{ W}\cdot\text{mm}^{-1}$ associated with 20.5 % power added efficiency and a linear power gain (G_p) of 4.2 dB is demonstrated for 70 nm gate length device. The device exhibits a maximum DC drain current density of $950 \text{ mA}\cdot\text{mm}^{-1}$ and a peak extrinsic transconductance ($g_{m \text{ Max}}$) of $300 \text{ mS}\cdot\text{mm}^{-1}$ at $V_{DS} = 6 \text{ V}$. A 100 GHz maximum intrinsic cutoff frequency f_T , and a maximum intrinsic oscillation frequency f_{Max} of 125 GHz are obtained from S-parameters measurement. This performance is very promising for HEMTs grown on Free-Standing GaN substrate.

Keywords: free-standing GaN, hydride vapor phase epitaxy (HVPE), AlGaN/GaN, high electron mobility transistor (HEMT), millimeter-wave power density

1. Introduction

Gallium Nitride (GaN) High Electron Mobility Transistor (HEMT) constitutes the best candidate for millimeter wave power applications [1], due to its remarkable material properties such as high breakdown voltage, high saturation velocity, and high thermal conductivity. Most AlGaN/GaN HEMT epilayers are grown on Silicon Carbide (SiC) substrate for high resistivity and good thermal management [2], [3], and on Silicon substrate (Si) because of its low-cost, large area availability, and compatibility with MOS technology [4]. However, during the epitaxial growth, many defects appear in the material (dislocations with density from 10^8 to 10^{10} cm^{-2}), because of the crystal lattice mismatch of 17% (4%) between GaN and Si (SiC) substrate. To this, is added a difference in

the thermal expansion coefficient of 54% and 25% with Si and SiC substrates respectively, which can induce noticeable tensile stress responsible for layer cracking. In this paper, the device is fabricated on AlGaN/GaN epilayer grown by Metal Organic Chemical Vapor Deposition (MOCVD) on Hydride Vapor Phase Epitaxy (HVPE) commercial Free-Standing Gallium Nitride (GaN) substrate. This structure presents the advantages of the direct growth of high crystalline quality GaN with threading dislocation density below 10^7 cm^{-2} [5], [6]. The goal of this study is to demonstrate the high microwave power performance at 40 GHz of HEMTs on GaN substrate.

Several studies have been conducted previously to fabricate high-frequency transistors on high quality GaN substrates.

An output power density of $9.4 \text{ W}\cdot\text{mm}^{-1}$ at 10 GHz [7], and $6.7 \text{ W}\cdot\text{mm}^{-1}$ at 4 GHz using back-barrier [8] are reported. With an AlN barrier, David J. Meyer et al. obtained $1 \text{ W}\cdot\text{mm}^{-1}$ at 40 GHz with a cutoff frequency f_T of 165 GHz and a 171 GHz maximum oscillation frequency [9]. Thus, it has been demonstrated that AlGaIn/GaN HEMT homo-epitaxial devices present relevant DC characteristics and microwave power performances [10]–[14]. Furthermore, beyond the expected benefit of better reliability on high crystal quality materials, further progress of performance is still achievable by improving the epilayer design and growth as well as the transistor process.

In this letter, DC and RF electrical performances are described and state of the art microwave performance such as a power density of $2 \text{ W}\cdot\text{mm}^{-1}$ at 40GHz are carried out demonstrating the capability of an AlGaIn/GaN HEMT grown on doped Free-Standing GaN substrate.

2. Material growth and device technology

2.1 Material growth

From commercial Hydride Vapor Phase Epitaxy (HVPE) Free-Standing (2-inches diameter) GaN substrates ($\rho \leq 30 \text{ m}\Omega\cdot\text{cm}$) supplied by Saint-Gobain Lumilog, a sufficiently thick and resistive $10 \mu\text{m}$ GaN buffer layer is grown by Metal Organic Chemical Vapor Deposition (MOCVD) in a close-coupled showerhead Aixtron reactor. This thick buffer is needed to minimize leakage current and to limit the coupling of the conductive substrate with the AlGaIn/GaN heterostructure, and thus lowering RF dielectric losses. As in ref [15], growth conditions are chosen to obtain $3 \mu\text{m}$ carbon rich resistive GaN layer before the growth of $7 \mu\text{m}$ unintentionally doped (UID) GaN. The HEMT active layers consist of a 11 nm thick $\text{Al}_{0.26}\text{Ga}_{0.74}\text{N}$ barrier capped with 3 nm thick in-situ grown SiN layer. A 1.5 nm thick AlN exclusion layer is used to reduce alloy scattering and to improve carrier confinement within the 2D electron gas (2DEG) (Fig. 1 (a)). The direct growth of AlGaIn/GaN layers permits the suppression of the nucleation layer, which is considered as a thermal barrier [16]. X-ray diffraction performed on the structure shows that the high quality of the free-standing GaN substrates is well replicated: full width at half maximum for the (002) and (302) rocking curves are $98''$ and $200''$ respectively.

This structure produces a 2DEG with a total charge density of $8.5 \times 10^{12} / \text{cm}^2$ and an electron mobility of $2200 \text{ cm}^2/\text{Vs}$ obtained from Hall effect measurement. This mobility and charge density translate to a 2DEG sheet resistance of $356 \Omega/\text{sq}$ at room temperature.

2.2 Device technology

The device fabrication starts with alignment marks made by Inductively Coupled Plasma (ICP) etching. Using a Cl_2/Ar

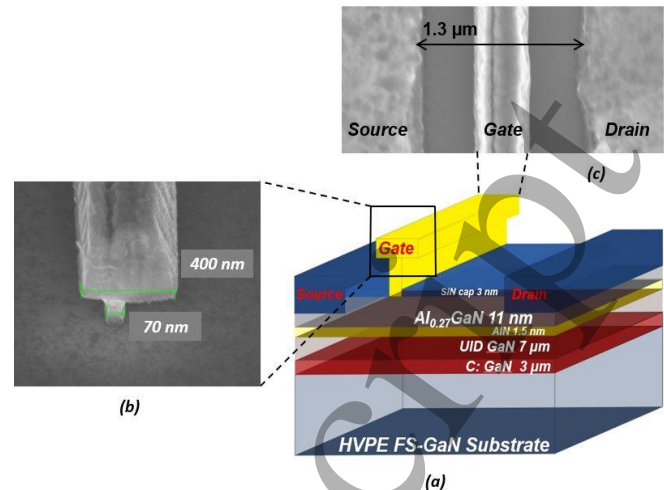


Fig. 1. (a) 3D schematic of the as-fabricated AlGaIn/GaN HEMT on Free-Standing GaN substrate before passivation with SiN, (b) SEM image after gate lift-off (c) SEM top view of the device after gate fabrication

plasma chemistry, alignment marks are etched to a depth of 650 nm. The process continues with the deposition of ohmic contacts metallization Ti/Al/Ni/Au (12/200/40/100 nm) by e-beam evaporation after in-situ-Argon (Ar) ion beam etching (IBE), where more than half of the barrier layer is etched to set the metallic sequential closer to the 2D conduction channel without degrading the UID-GaN layer. This is followed by rapid thermal annealing (RTA) at $850 \text{ }^\circ\text{C}$ for 30 s under nitrogen atmosphere. Then, devices are isolated by N^+ ion multiple implantations. An average contact resistance as low as $R_C = 0.34 \Omega\cdot\text{mm}$ is measured by a transmission line model on different patterns. T-shaped gate based on Ni/Au (40/300 nm) evaporated metallization with 70 nm footprint (Fig. 1 (b)) are patterned by electron-beam lithography process using optimized (PMMA/COPO/PMMA) tri-layer resist stack. $400 \text{ }^\circ\text{C}$ annealing for 20 min under nitrogen atmosphere is done in order to improve Schottky contact behavior by reducing the trapping phenomena under the gate [17]. Then, Si_3N_4 passivation is performed by Plasma-Enhanced Chemical Vapor Deposition (PECVD) at $340 \text{ }^\circ\text{C}$. Finally, a Ti/Au stack is deposited by evaporation to access transistor contacts. Device under test (DUT) in this paper features a two-finger configuration with a gate length $L_g = 70 \text{ nm}$, a gate width $W = 2 \times 50 \mu\text{m}$ and source-to-drain spacing $L_{SD} = 1.3 \mu\text{m}$. Fig. 1 (b) and Fig. 1 (c) shows a Scanning Electron Microscope (SEM) view of the T-shaped gate obtained on a device with 500 nm source-to-gate spacing.

3. Measurements and results

3.1 DC Characteristics

Fig. 2 shows the output $I_{DS}(V_{DS})$ characteristics for a device featuring 2 fingers of $50 \mu\text{m}$ each, with a gate-to-drain spacing $L_{DG} = 730 \text{ nm}$, and a source-to-gate spacing $L_{GS} = 500 \text{ nm}$. From these measurements, a maximum DC current density $I_{DS \text{ Max}}$ of $950 \text{ mA}\cdot\text{mm}^{-1}$ is reached at $V_{GS} = 1 \text{ V}$, associated with an ON-resistance of $3 \Omega\cdot\text{mm}$.

As shown in Fig. 3, for different V_{GS} ranging from -6 V to 0 V , an extrinsic transconductance $g_{m, \text{ext}}$ peak of $300 \text{ mS}\cdot\text{mm}^{-1}$ at $V_{GS} = -2.5 \text{ V}$ and $V_{DS} = 6 \text{ V}$ is obtained. A threshold voltage V_{th} of -3.5 V is deduced from the transfer characteristic. The gate leakage current is as low as $3.10^{-7} \text{ A}/\text{mm}$. The I_{ON}/I_{OFF} ratio of drain current I_{DS} is above 10^6 .

3.2 RF Characteristics

The scattering S_{ij} parameters are measured in the 250 MHz to 67 GHz frequency range, using a Vector Network Analyzer (VNA). The calibration procedure is performed on wafer, using a Line-Reflect-Reflect-Match (LRRM) procedure. The current gain modulus ($|H_{21}|$) and Mason's unilateral gain (U) are extracted from S-parameters versus frequency measurement. Using Open-Short patterns, the inductive and capacitive pad contributions are de-embedded. The current transition frequency (f_T) and the maximum oscillation frequency (f_{Max}) are directly extracted from the first order linear frequency regression (-20 dB/decade) plots of $|H_{21}|$ and U respectively. These figures of merit are depicted in Fig. 4 for a biasing at $V_{GS} = -2.5 \text{ V}$ and $V_{DS} = 6 \text{ V}$, corresponding to the extrinsic transconductance peak.

An intrinsic current gain cut-off frequency f_T of 100 GHz associated with a maximum oscillation frequency f_{Max} of 125 GHz are achieved. These values are obtained thanks to an optimized device processing (T-shaped gate), and also to the high material quality, by using thin barrier (11 nm) and thick GaN buffer on the Free-Standing GaN substrate. Optimization of thickness and carbon doping level of the C-doped GaN layer may further improve these results. It must be a trade-off between crystal quality and buffer isolation [18], [19].

3.3 Microwave power measurements

Large-signal microwave power measurement was performed at 40 GHz . It is based on an active load pull setup under CW conditions with a large-signal network analyser (LSNA) working up to 50 GHz . At $V_{DS} = 10 \text{ V}$ and $I_{DS} = 300 \text{ mA}\cdot\text{mm}^{-1}$ corresponding to class AB operation, the optimal load impedance is $\Gamma_{load} = 0.75 \angle 85^\circ$. At this condition, the device exhibits an output power density (P_{out}) of $1.2 \text{ W}\cdot\text{mm}^{-1}$ associated with a maximum power-added efficiency (PAE) of 26.2% and a linear gain of 5 dB . Measurement was also carried out at $V_{DS} = 15 \text{ V}$ and $I_{DS} = 300 \text{ mA}\cdot\text{mm}^{-1}$ (Fig. 5). For $\Gamma_{load} = 0.7 \angle 80^\circ$, an output power density of $2 \text{ W}\cdot\text{mm}^{-1}$ associated with a maximum power-added efficiency (PAE) of 20.5% , and a linear gain of 4.2 dB are achieved.

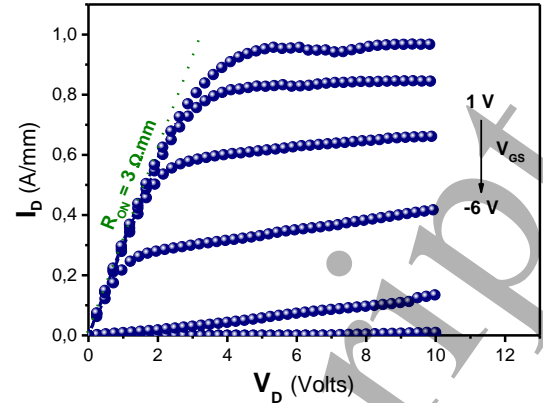


Fig. 2. $I_{DS}(V_{DS})$ characteristics for a $2 \times 50 \times 0.07 \mu\text{m}^2$ AlGaIn/GaN HEMT on Free-Standing GaN substrate.

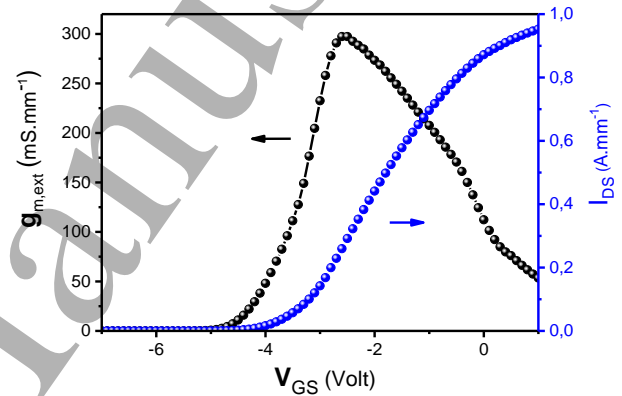


Fig. 3. Transfer characteristics at $V_{DS} = 6 \text{ V}$ for a $2 \times 50 \times 0.07 \mu\text{m}^2$ AlGaIn/GaN HEMT on Free-Standing GaN substrate.

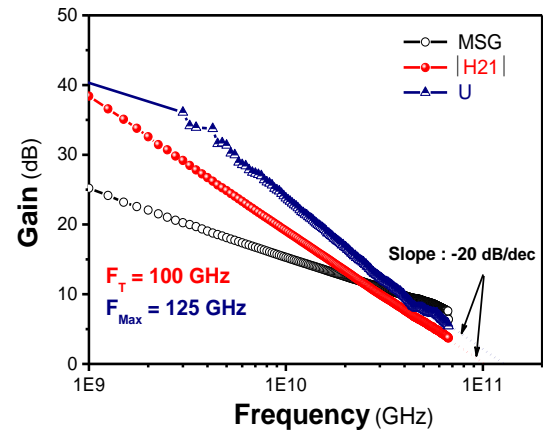


Fig. 4. Current gain modulus $|H_{21}|$, Mason's unilateral gain (U) and maximum Stable Gain (MSG) versus frequency for a $2 \times 50 \times 0.07 \mu\text{m}^2$ AlGaIn/GaN HEMT on Free-Standing GaN substrate at $V_{GS} = -2.5 \text{ V}$, $V_{DS} = 6 \text{ V}$

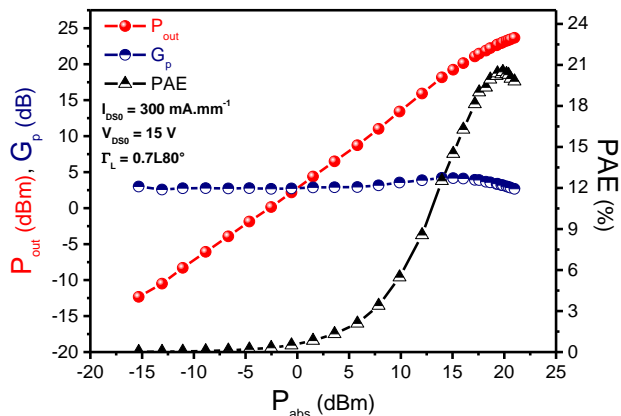


Fig. 5. Output power, power gain and power added efficiency versus absorbed power at 40 GHz for a $2 \times 50 \times 0.07 \mu\text{m}^2$ AlGaIn/GaN HEMT on Free-Standing GaN substrate.

Up to now, this result constitutes the state-of-the-art large signal at 40 GHz for AlGaIn/GaN HEMTs on Free-Standing GaN substrate.

4. Conclusion

AlGaIn/GaN HEMT grown on Free-Standing GaN substrate are fabricated. Attractive small-signal and RF power performances are demonstrated for a $2 \times 50 \times 0.07 \mu\text{m}^2$ device. A record output power density for HEMT on Free-Standing GaN substrate, as high as $2 \text{ W}\cdot\text{mm}^{-1}$ is obtained at 40 GHz associated with a PAE of 20.5 % and a linear power gain of 4.2 dB. The transistor exhibits intrinsic cut-off frequencies $f_T = 100 \text{ GHz}$ and $f_{\text{Max}} = 125 \text{ GHz}$ at $V_{\text{GS}} = -2.5 \text{ V}$ and $V_{\text{DS}} = 6 \text{ V}$. These results show the capability of AlGaIn/GaN HEMT based on Free-Standing GaN substrate for high millimeter-wave power applications.

Acknowledgements

This work has been supported by the cluster of Excellence GaNeX which belongs to the public funded 'Investissements d'Avenir' (ANR-11-LABX-0014) program managed by the French Research National Agency, and also by the French Renatech network.

References

[1] T. Palacios *et al.*, « High-power AlGaIn/GaN HEMTs for Ka-band applications », *IEEE Electron Device Lett.*, vol. 26, n° 11, p. 781-783, nov. 2005.

[2] V. D. Giacomo-Brunel *et al.*, « Industrial 0.15- μm AlGaIn/GaN on SiC Technology for Applications up to Ka Band », *13th European Microwave Integrated Circuits Conference (EuMIC)*, p. 1-4, 2018.

[3] R. Gaska *et al.*, « High-temperature performance of AlGaIn/GaN HFETs on SiC substrates », *IEEE Electron Device Lett.*, vol. 18, n° 10, p. 492-494, oct. 1997.

[4] D. Kim *et al.*, « Ka-Band MMIC Using AlGaIn/GaN-on-Si With Recessed High- κ Dual MIS Structure », *IEEE Electron Device Lett.*, vol. 39, n° 7, p. 995-998, juill. 2018.

[5] D. Gogova *et al.*, « High-Quality 2nd Bulk-Like Free-Standing GaN Grown by Hydride Vapour Phase Epitaxy on a Si-doped Metal Organic Vapour Phase Epitaxial GaN Template with an Ultra-Low Dislocation Density », *Jpn. J. Appl. Phys.*, vol. 44, n° 3R, p. 1181, mars 2005.

[6] S. M. Eichfeld *et al.*, « Dual temperature process for reduction in regrowth interfacial charge in AlGaIn/GaN HEMTs grown on GaN substrates », *Phys. Status Solidi C*, vol. 8, n° 7-8, p. 2053-2055, 2011.

[7] K. K. Chu *et al.*, « 9.4-W/mm power density AlGaIn-GaN HEMTs on free-standing GaN substrates », *IEEE Electron Device Lett.*, vol. 25, n° 9, p. 596-598, sept. 2004.

[8] S. W. Kaun *et al.*, « Reduction of carbon proximity effects by including AlGaIn back barriers in HEMTs on free-standing GaN », *Electron. Lett.*, vol. 49, n° 14, p. 893-895, juill. 2013.

[9] D. J. Meyer *et al.*, « High Electron Velocity Submicrometer AlN/GaN MOS-HEMTs on Freestanding GaN Substrates », *IEEE Electron Device Lett.*, vol. 34, n° 2, p. 199-201, 2013.

[10] N. Killat *et al.*, « Reliability of AlGaIn/GaN high electron mobility transistors on low dislocation density bulk GaN substrate: Implications of surface step edges », *Appl. Phys. Lett.*, vol. 103, n° 19, p. 193507, nov. 2013.

[11] A. Fontserè *et al.*, « Bulk Temperature Impact on the AlGaIn/GaN HEMT Forward Current on Si, Sapphire and Free-Standing GaN », *ECS Solid State Lett.*, vol. 2, n° 1, p. P4-P7, janv. 2013.

[12] D. Zhang *et al.*, « Reliability Improvement of GaN Devices on Free-Standing GaN Substrates », *IEEE Trans. Electron Devices*, vol. 65, n° 8, p. 3379-3387, 2018.

[13] D. F. Storm *et al.*, « Microwave performance and structural characterization of MBE-grown AlGaIn/GaN HEMTs on low dislocation density GaN substrates », *J. Cryst. Growth*, vol. 305, n° 2, p. 340-345, juill. 2007.

[14] J. K. Gillespie *et al.*, « Uniformity of dc and rf performance of MBE-grown AlGaIn/GaN HEMTs on HVPE-grown buffers », *Solid-State Electron.*, vol. 47, n° 10, p. 1859-1862, oct. 2003.

[15] E. Frayssinet *et al.*, « Influence of metal-organic vapor phase epitaxy parameters and Si(111) substrate type on the properties of AlGaIn/GaN HEMTs with thin simple buffer », *physica status solidi (a)*, 2017.

[16] G. J. Riedel *et al.*, « Reducing Thermal Resistance of AlGaIn/GaN Electronic Devices Using Novel Nucleation Layers », *IEEE Electron Device Lett.*, vol. 30, n° 2, p. 103-106, févr. 2009.

[17] J. Gerbedoen *et al.*, « Performance of Unstuck - Gate AlGaIn/GaN HEMTs on (001) Silicon Substrate at 10 GHz », *European Microwave Integrated Circuit Conference*, p. 330-333, 2008.

[18] P. Gamarra *et al.*, « Optimisation of a carbon doped buffer layer for AlGaIn/GaN HEMT devices », *J. Cryst. Growth*, vol. 414, p. 232-236, mars 2015.

[19] D. F. Storm *et al.*, « Proximity effects of beryllium-doped GaN buffer layers on the electronic properties of epitaxial AlGaIn/GaN heterostructures », *Solid-State Electron.*, vol. 54, n° 11, p. 1470-1473, nov. 2010.